

# Intergranular pinning potential and critical current in the magnetic superconductor $\text{RuSr}_2\text{Gd}_{1.5}\text{Ce}_{0.5}\text{Cu}_2\text{O}_{10}$

M. G. das Virgens,<sup>1,2</sup> S. García,<sup>1,3,\*</sup> M. A. Continentino,<sup>2</sup> and L. Ghivelder<sup>1</sup>

<sup>1</sup>*Instituto de Física, Universidade Federal do Rio de Janeiro, Caixa Postal 68528, Rio de Janeiro, RJ, 21941-972, Brazil*

<sup>2</sup>*Instituto de Física, Universidade Federal Fluminense, Campus da Praia Vermelha, Niterói, RJ, 24210-340, Brazil*

<sup>3</sup>*Laboratorio de Superconductividad, Facultad de Física-IMRE, Universidad de La Habana, San Lázaro y L, Ciudad de La Habana 10400, Cuba*

(Received 19 July 2004; published 28 February 2005)

The intergranular pinning potential  $U$  and the critical current density  $J_C$  for polycrystalline  $\text{RuSr}_2\text{Gd}_{1.5}\text{Ce}_{0.5}\text{Cu}_2\text{O}_{10}$  ruthenate-cuprate were determined at zero magnetic field and temperature through the frequency shift in the peak of the imaginary part of the ac magnetic susceptibility,  $\chi''$ . A critical state model, including a flux creep term, was found to accurately describe the  $\chi''$  behavior. The obtained values,  $U(H=0, T=0) \cong 30$  meV and  $J_C(H=0, T=0) \cong 110$  A/cm<sup>2</sup> are about two orders of magnitude and four times lower, respectively, in comparison with the high- $T_C$  cuprate  $\text{YBa}_2\text{Cu}_3\text{O}_7$ . These results were ascribed to the effects of the Ru magnetization on the connectivity of the weak-linked network, giving an intrinsic local field at the junctions of  $\sim 15$  Oe. The impact on  $J_C$  is less intense because of the small average grain radius ( $\sim 1$   $\mu\text{m}$ ). The intragranular London penetration length at  $T=0$  [ $\lambda_L(0) \cong 2$   $\mu\text{m}$ ] was derived using a Kim-type expression for the field dependence of  $J_C$ . A possible source for the large value of  $\lambda_L$  in comparison to the high- $T_c$  cuprates is suggested to come from a strong intragrain granularity, due to structural domains of coherent-rotated  $\text{RuO}_6$  octahedra separated by antiphase boundaries.

DOI: 10.1103/PhysRevB.71.064520

PACS number(s): 74.72.-h, 74.25.Ha, 74.25.Sv

## I. INTRODUCTION

The coexistence of ferromagnetic (FM) long-range order of the Ru moments with a superconducting (SC) state in the ruthenate-cuprates  $\text{RuSr}_2\text{RCu}_2\text{O}_8$  (Ru-1212) and  $\text{RuSr}_2(\text{R}, \text{Ce})_2\text{Cu}_2\text{O}_{10}$  (Ru-1222), where  $\text{R}=\text{Gd}, \text{Eu}$ , has been intensively studied in recent years.<sup>1-8</sup> Among several major open issues, the interplay between the transport properties and magnetism has received a great deal of attention.<sup>9-12</sup> On the other hand, there are few reports on the intergrain properties, which exhibit very interesting features. The broad resistive SC transition ( $\Delta T_{\text{SC}} \approx 15-20$  K) observed in good quality Ru-1212 ceramic samples has been consistently explained in terms of a strong intergrain contribution and spontaneous vortex phase formation in the grains, as evidenced through microwave resistivity measurements in powders dispersed in an epoxy resin.<sup>13</sup> An abrupt reduction in the suppression rate of the intergranular flux activation energy with the increase in magnetic field has been observed at  $H=0.1$  T in polycrystalline Ru-1212, through a study of the  $I$ - $V$  characteristic curves.<sup>14</sup> This behavior has been ascribed to a spin-flop transition of the Ru sublattice, leading to a decrease of the effective local field at the junctions. In addition, a preliminary report<sup>15</sup> on  $I$ - $V$  curves for Ru-1222 suggests that the low values obtained for the intergranular current density  $J_C$  is possibly related to its magnetic behavior, indicating that more investigation is needed to clarify this point. The peak of the SC intergrain transition, as determined from the derivative of the resistive curves, is quite intense and narrow in both ruthenate-cuprate systems.<sup>16</sup> This result is at variance with the high- $T_c$  cuprates, exhibiting a smeared intergrain peak of small amplitude as a consequence of a broad-in-temperature phase-lock process

across a wide distribution of link qualities. The results for the ruthenate-cuprates have been interpreted as a consequence of the effects of the Ru magnetization on the grain boundaries, in such a way that the intergrain percolation occurs only through a fraction of high quality junctions.<sup>16</sup> These reports clearly show that the magnetization in the grains leaves a sizable effect in the connectivity of the weak link network. Whether this unique feature of the ruthenate-cuprates changes the essentials of the intergrain properties in comparison to the high- $T_c$  superconductors remains an open issue; a quantitative determination of the parameters characterizing the intergrain coupling in these compounds is still lacking.

Since the early works in the high- $T_c$  superconductors, ac magnetic susceptibility has proved to be a useful tool to characterize their granular properties.<sup>17-19</sup> In particular, a critical state model for granular superconductors was used to calculate the temperature, and both ac and dc magnetic field dependence of the complex susceptibility,  $\chi' = i + \chi''$ , for sintered bulk samples of  $\text{YBa}_2\text{Cu}_3\text{O}_7$  (YBCO),<sup>20-22</sup>  $(\text{Bi}, \text{Pb})_2\text{Sr}_2\text{Ca}_2\text{Cu}_3\text{O}_{10}$  and  $\text{Bi}_2\text{Sr}_2\text{CaCu}_2\text{O}_8$ ,<sup>23</sup> with excellent results. In this paper we present detailed measurements of the ac magnetic susceptibility as a function of frequency  $f$  and amplitude  $h_{\text{ac}}$  of the driving field in polycrystalline  $\text{RuSr}_2\text{Gd}_{1.5}\text{Ce}_{0.5}\text{Cu}_2\text{O}_{10-\delta}$ . We show that the simple models proposed to describe the dependence on these parameters of the imaginary part of the susceptibility,  $\chi''$ , in the conventional cuprates<sup>23-26</sup> quantitatively accounts for the behavior of the dissipation peak in Ru-1222. Nevertheless, the parameters characterizing the intergrain properties, as the pinning potential depth, the full penetration field, and the critical current density, are considerably lower in Ru-1222 as compared to the high- $T_c$  cuprates. We propose that

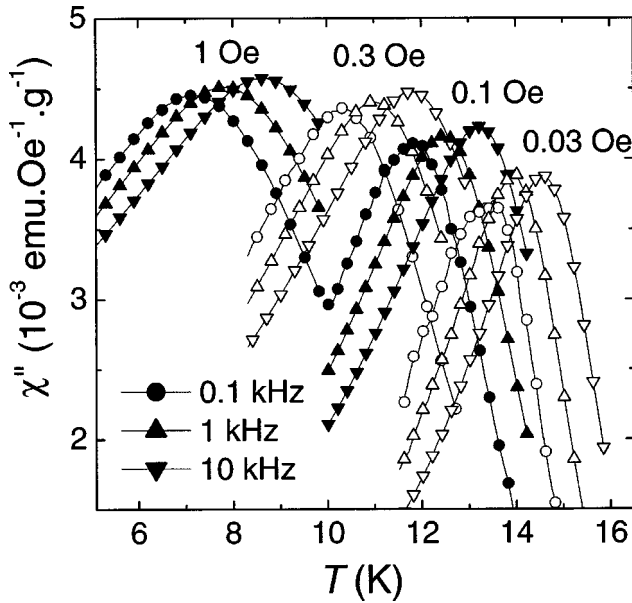


FIG. 1. Temperature dependence of the imaginary part of the ac magnetic susceptibility,  $\chi''$ , for Ru-1222 using different amplitudes and frequencies of the driving field. Selected curves for  $f=0.1, 1,$  and  $10$  kHz are shown. For the sake of clarity not all measured data points are plotted.

these results are due to effects of the Ru magnetization within the grains on the connectivity of the weak link network.

## II. EXPERIMENTAL

Polycrystalline  $\text{RuSr}_2\text{Gd}_{1.5}\text{Ce}_{0.5}\text{Cu}_2\text{O}_{10-\delta}$  (Ru-1222) was prepared by conventional solid-state reaction. Details on sample preparation, microstructure, and the resistive SC transition can be found elsewhere.<sup>16</sup> The room temperature x-ray diffraction pattern corresponds to Ru-1222, with no spurious lines being observed. Scanning electron microscopy (SEM) revealed a dense packing of grains, with an average grain radius  $\cong 1 \mu\text{m}$ , leading to a well-connected microstructure. The intragrain SC transition temperature is  $T_{\text{SC}}=22$  K.<sup>16</sup> Bars of  $\approx 10 \times 1.7 \times 1.7 \text{ mm}^3$  were cut from the sintered pellet. The real ( $\chi'$ ) and imaginary ( $\chi''$ ) parts of the ac magnetic susceptibility were measured in a Quantum Design PPMS system, with ac amplitudes  $h_{\text{ac}}=0.03, 0.1, 0.3,$  and  $1$  Oe, and frequencies  $f=35, 100, 350$  Hz, and  $1.0, 3.5,$  and  $10$  kHz. For  $f=1$  kHz, the curves with  $h_{\text{ac}}=0.01$  and  $3$  Oe were also measured. The  $\chi''$  peak temperature,  $T_p$ , was determined by conventional numerical derivation of the experimental curves.<sup>27</sup>

## III. RESULTS

Figure 1 shows the imaginary part of the ac susceptibility of Ru-1222,  $\chi''(h_{\text{ac}}, T, f)$ . For the sake of clarity, only selected curves are presented, for low-, medium-, and high-frequency values. The peaks in  $\chi''$  are grouped in four sets of data, corresponding to the ac amplitudes  $h_{\text{ac}}$  used. Higher  $h_{\text{ac}}$  values move the curves to lower

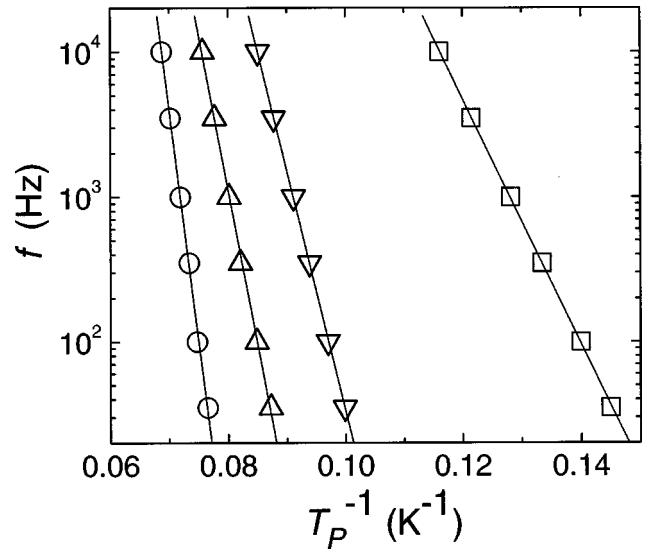


FIG. 2. Logarithmic plot of the ac driving frequency,  $f$ , vs the reciprocal of the  $\chi''$ -peak temperature,  $T_p^{-1}$ , for different amplitudes  $h_{\text{ac}}$ ; from left to right  $h_{\text{ac}}=0.03, 0.1, 0.3,$  and  $1$  Oe. The continuous lines are linear fittings.

temperatures. Inside each set of data, the peaks are shifted to higher temperatures as  $f$  is increased. Typically, the total temperature shift,  $\Delta T_p$ , for the measuring  $\Delta f$  interval, is approximately 2 K. In Fig. 2 we show a logarithmic plot of  $f$  vs  $1/T_p$  for different  $h_{\text{ac}}$  values. The points clearly follow a linear dependence, corresponding to an Arrhenius-type expression  $f=f_0\exp(E_f/kT_p)$ , where  $E_f$  plays the role of an activation energy associated to the frequency effects,  $f_0$  is a characteristic frequency, and  $k$  is the Boltzmann constant. The activation energies calculated from the slopes of the linear fits of the Arrhenius plots are in the 8–30 meV range. The inset of Fig. 3 shows  $E_f$  as a function of  $h_{\text{ac}}$  using a logarithmic scale. For comparisons with the results obtained for the high- $T_c$  cuprates, we extrapolated to  $h_{\text{ac}}=0.02$  Oe ( $\cong 1$  A/m rms), giving  $E_f(h_{\text{ac}}=0.02 \text{ Oe}) \cong 30$  meV.

The variation in  $T_p$  for different  $h_{\text{ac}}$  amplitudes, measured with  $f=1$  kHz, is plotted in Fig. 3. The largest measuring amplitude for which a peak is observed is  $h_{\text{ac}}=3$  Oe, with  $T_p=2.7$  K. A polynomial fitting (continuous line) yield  $h_{\text{ac}}(T_p=0)=5$  Oe. This is the full penetration field  $H^*(0)$  of the bar-shaped sample at  $T=0$  for  $f=1$  kHz.

## IV. DISCUSSION AND CONCLUSIONS

As already mentioned, the critical state model has been successfully used to characterize the granular properties of high- $T_c$  superconductors. In particular, it was shown that a flux creep term added to the current density term in the critical state equation accurately accounts for the shift in the  $\chi''$  peak to higher temperatures with increasing frequency of the ac field.<sup>23–26</sup> In the following, we briefly review the essential ideas of this approach necessary to conduct the discussion; details can be found in the previously mentioned reports. We compare our results with bulk yttrium barium copper oxide

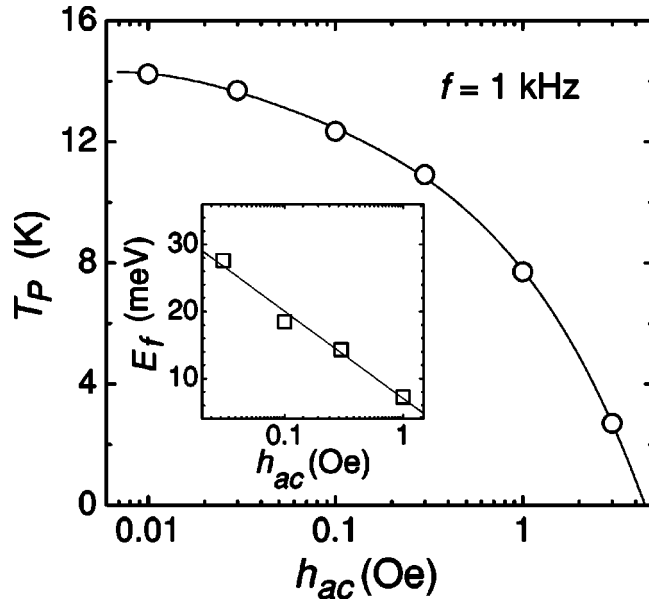


FIG. 3.  $\chi''$ -peak temperature,  $T_p$ , plotted as a function of  $\log(h_{ac})$ . The continuous line is a polynomial fitting, which yields  $h_{ac}=5$  Oe for  $T_p=0$ . Inset: the activation energy,  $E_f$ , determined from the slopes of the linear fittings in Fig. 2, plotted as a function of  $h_{ac}$ . The extrapolation to  $h_{ac}=0.02$  Oe ( $\sim 1$  A/m rms), gives  $E_f(h_{ac}=0.02 \text{ Oe}) \cong 30$  meV.

(YBCO), for which more detailed data is available. One interesting prediction of the model is that larger shifts should be observed with decreasing average grain size and critical current density at the intergrain junctions.<sup>25</sup> Since the connectivity of the weak link network in Ru-1222 is expected to be affected by the Ru magnetization in the grains and the Ru-1222 average grain radius  $R_g \approx 1 \mu\text{m}$  is lower than those reported for the YBCO sample ( $\sim 7\text{--}10 \mu\text{m}$ ), this compound is a suitable material to verify this point. The five-times larger temperature shift  $\Delta T_p$  due to a frequency variation, observed for Ru-1222 as compared with YBCO [ $\Delta T_p(\text{YBCO}) \sim 0.4 \text{ K}$ ]<sup>25</sup> for the same  $\Delta f$  interval confirms these predictions. It is worth mentioning that  $H^*(0)$  for the Ru-1222 bulk sample is reduced by a factor of four [ $\Delta H^*(0)_{\text{YBCO}} = 20 \text{ Oe}$  for  $f=1 \text{ kHz}$ ],<sup>26</sup> also pointing to a weak intergrain connectivity. The dense, well-connected microstructure observed in the SEM images indicates that this poor intergranular coupling is not related to small contact areas between the grains.

The shift in  $T_p$  can be understood in terms of a frequency dependent effective pinning. As the frequency is increased, the intergranular vortices have less time to creep into the superconductor during each ac cycle. Then, in order to obtain the full penetration condition, a weaker intergranular pinning force density is needed to compensate for a less efficient creep. Since the pinning force density weakens with increasing temperature,  $T_p$  must increase with the rise in frequency.

For the calculation of the intergranular critical current density the critical state equation for an infinite slab is used<sup>28,29</sup>

$$dH(x)/dx = J_C(H, T) = \frac{F_p(H, T)}{|B(x)|}, \quad (1)$$

where  $B(x)$  is the local macroscopic flux density due to the external field,  $x$  is the coordinate perpendicular to the slab, and  $F_p(H, T)$  is the pinning force density given by

$$F_p(H, T) = \frac{1}{V_b d} \left[ U(H, T) + kT \ln\left(\frac{f}{f_0}\right) \right], \quad (2)$$

where  $U(H, T)$  is the pinning depth potential,  $V_b$  is the flux bundle volume and  $d$  half the width of the pinning potential well. The second term in Eq. (2) represents the flux creep contribution. The flux bundle  $V_b$  for intergranular vortices is assumed to contain a single flux quantum  $\Phi_0$ , and the pinning sites are supposed to be located between the corners of adjacent grains. For granular material approximated by a regular array of junctions and cubic grains it is obtained<sup>25</sup>

$$V_b = \frac{2R_g \Phi_0}{|B(x)|}, \quad (3)$$

where  $R_g$  represents the average grain radius. The half width  $d$  of the pinning potential is equated to  $R_g$ . Inserting Eqs. (2) and (3) into Eq. (1) and evaluating for  $H=0$  and  $T=0$  one obtains

$$J_C(0, 0)_{\text{Ru}} = \frac{U(0, 0)}{2R_g^2 \Phi_0}, \quad (4)$$

where  $J_C(0, 0)_{\text{Ru}}$  is the critical current density at the zero external field of a weak-link network with its connectivity affected by the intrinsic Ru magnetization; we will return to this point below.

Müller<sup>25</sup> showed that in the zero-field limit  $E_f(T_p, h_{ac} \cong 0) \cong U(0, 0)$ . The procedure adopted in the studies of high- $T_c$  cuprates is to extrapolate the  $E_f$  vs logarithm  $h_{ac}$  plot to the low-field region. Since the extrapolation to exactly  $h_{ac}=0$  is not possible, due to the divergence of the logarithmic function, the usual practice is to take  $h_{ac}=1 \text{ A/m(rms)} \cong 0.02 \text{ Oe}$  as a reference “low-field criterion,”<sup>23–25</sup> which is close to our lowest  $h_{ac}$  amplitude used. The extrapolation in Fig. 3 gives  $U(0, 0) \cong 30 \text{ meV}$ . This value represents a 400-fold decrease in comparison to YBCO [ $U(0, 0)_{\text{YBCO}} \cong 12 \text{ eV}$ ]. Using Eq. (4) with  $U(0, 0) \cong 30 \text{ meV}$  we obtain  $J_C(0, 0)_{\text{Ru}} = 110 \text{ A/cm}^2$ , a value six times lower in comparison to YBCO.<sup>26</sup> It is important to notice that the decreasing factor for  $J_C(0, 0)$ , as determined from the frequency shift, is similar to that for  $H^*(0)$ , which was obtained from the  $h_{ac}$  dependence of the  $\chi''$  peaks. The huge effect in  $U(0, 0)$  is due to a strong weakening in the connectivity of the intergranular network as a consequence of the Ru magnetization in the grains. The impact on  $J_C(0, 0)_{\text{Ru}}$  is less intense due to the small average grain size.

The value of  $J_C(0, 0)_{\text{Ru}}$  can be calculated by an alternative approach, still within the framework of the critical state model. Equation (1) can be written as

$$dH(x)/dx = J_C(0, T) \frac{H_0/2}{|H(x)| + H_0/2} + \frac{kT}{2R_g^2 \Phi_0} \ln \frac{f}{f_0}, \quad (5)$$

where the dependence of  $J_C$  on the local magnetic field  $H(x)$  is modeled by a Kim-type envelope of the Fraunhofer patterns associated to the distribution of junction qualities in the polycrystal. Here,  $H_0 = \Phi_0 / \mu_0 A_J$ , where  $\mu_0$  is the permeability of free space,  $A_J = 2R_g [2\lambda_L(T)]$  is the field-penetrated junction area, and  $\lambda_L(T)$  is the intragrain London penetration length. Evaluating Eq. (5) for the full penetration condition of the bar by an external field at  $T=0$  and integrating, we obtain

$$-\frac{H^{*2}(0)}{2H_0(0)} - H^*(0) + J_C(0, 0)_{\text{Ru}} \left(\frac{a}{2}\right) = 0, \quad (6)$$

where  $a$  is the thickness of the bar.

The use of Eq. (6) for the calculation of  $J_C(0, 0)_{\text{Ru}}$  requires the knowledge of  $\lambda_L(0)$ . However, it must be kept in mind that the intragrain London penetration length has some peculiarities in the ruthenate-cuprates. It has been demonstrated for Ru-1222 that the intragrain superfluid density  $1/\lambda_L^2$  does not follow by far the linear correlation with  $T_{\text{SC}}$  observed for homogeneous cuprates.<sup>6</sup> Also, it was found that  $\lambda_L$  is very sensitive to the partial pressure of oxygen during the final annealing, varying between 0.4  $\mu\text{m}$  ( $T_{\text{SC}}=40$  K) and 1.8  $\mu\text{m}$  ( $T_{\text{SC}}=17$  K).<sup>6</sup> For Ru-1212, samples with intragrain transition temperatures higher than 20 K show  $\lambda_L$  at 5 K as large as 2–3  $\mu\text{m}$ .<sup>30</sup> Thus, there is considerable uncertainty in the choice of the appropriate value of  $\lambda_L$  to determine  $J_C(0, 0)_{\text{Ru}}$  in our sample using Eq. (6). Instead, we look for a confirmation of the validity of the critical state model by taking the  $J_C(0, 0)_{\text{Ru}}$  value obtained from the frequency shift, and derive  $\lambda_L(0)$ . Taking  $J_C(0, 0)_{\text{Ru}}=110$  A/cm<sup>2</sup>,  $R_g=1$   $\mu\text{m}$ ,  $H^*(0)=5$  Oe, and  $a=1.7$  mm, we obtained  $\lambda_L(0)=2.2$   $\mu\text{m}$ , in good agreement with the value  $\lambda_L(5\text{ K})=1.8$   $\mu\text{m}$  reported for Ru-1222 ceramic with an intragrain transition temperature  $T_{\text{SC}}=17$  K (near to our value of  $T_{\text{SC}}=22$  K) through the particle-size dependence of the real part of the susceptibility.<sup>6</sup> We remark that  $\lambda_L(0)$  is larger in comparison to YBCO and other optimally doped high- $T_C$  cuprates, and comparable to the average grain size of Ru-1222. This should be related not only to the underdoped character of the ruthenate-cuprates, as revealed by Hall effect and thermopower measurements,<sup>9,10</sup> but also to a very distinctive feature of these compounds. Both Ru-1212 and Ru-1222 exhibit structural domains of coherent rotated  $\text{RuO}_6$  octahedra, separated by antiphase boundaries with local distortions and defects.<sup>2</sup> This characteristic has been proposed to be the source of the strong intragrain granularity observed in these compounds, with the boundaries acting as intragrain Josephson junctions between the structural domains.<sup>16</sup> Within this scenario, the magnetic field penetrates the grains not only through their crystallographic borders but also through the antiphase boundaries, increasing the penetrated volume and leading to an enhanced effective  $\lambda_L$  and to a small and sometimes missing Meissner

signal. Therefore, the obtained  $\lambda_L(0)$  provides a reliable estimate, and confirms the validity of the critical state approach.

Finally, we address the magnitude of the local field at the intergranular junctions due to the Ru magnetization,  $H_{\text{Ru}}$ . The use of the critical state model, leading to a decreasing field profile in the ceramic as its center is approached, is valid only if the external field is comparable to  $H_{\text{Ru}}$ . In the case where  $h_{\text{ac}}$  is much smaller than  $H_{\text{Ru}}$ , its effect on the connectivity of the weak link network is negligible, and no amplitude dependence for the position of the  $\chi''$  peaks would be observed. In other words, a large  $H_{\text{Ru}}$  will result in a flat intrinsic field profile unaffected by  $h_{\text{ac}}$ . Magnetic fields of the order of 600–700 Oe have been measured by muon spin rotation<sup>3</sup> and Gd-electron paramagnetic resonance<sup>31</sup> in sites located near to the  $\text{RuO}_2$  layers. However, the dipolar field rapidly decays with distance, and the local field at the junctions can be considerably smaller. Defects and imperfections in the region of the intergrain boundaries can locally affect the magnetic order of the Ru moments, diminishing the effective field. An estimation of  $H_{\text{Ru}}$  can be performed using the value reported for the intergrain critical current in the isomorphous nonferromagnetic Nb-1222 compound ( $J_{C\text{ Nb}}=1545$  A/cm<sup>2</sup> at  $T=5$  K).<sup>15</sup> Assuming similar superconducting properties, and keeping the Kim-type model to account for the dependence of  $J_C$  with the local magnetic field we can write

$$J_C(H_{\text{ext}}, T=0)_{\text{Ru}} = J_C(H_{\text{ext}}=0, T=5\text{ K})_{\text{Nb}} \times \frac{H_0/2}{|H(x) + H_{\text{Ru}}| + (H_0/2)}, \quad (7)$$

where  $H(x)$  and  $H_{\text{Ru}}$  must be added, taking into account their relative orientations. Evaluating Eq. (7) for  $H_{\text{ext}}=h_{\text{ac}}=0$  and taking  $\lambda_L(0)=2.2$   $\mu\text{m}$ ,  $R_g=1$   $\mu\text{m}$  [giving  $H_0(0)=2.3$  Oe] and  $J_C(0, 0)_{\text{Ru}}=110$  A/cm<sup>2</sup>, we obtain  $H_{\text{Ru}} \cong 15$  Oe. An intrinsic local field at the intergranular junctions of this magnitude is large enough to greatly affect the connectivity of the network, but still leave it sensitive to the action of external oscillating fields of a few Oersted.

In summary, a detailed study of  $\chi''(h_{\text{ac}}, f, T)$  curves in polycrystalline Ru-1222 allowed a quantitative characterization of the intergrain coupling in a ruthenate-cuprate. The intergranular pinning potential and the critical current density at zero field and temperature were determined. A critical state model, including flux creep effects, was found to properly describe the  $\chi''$  behavior. The pinning potential showed a very strong decrease in comparison to the high- $T_C$  cuprates. This is ascribed to the effects of the Ru magnetization in the grains on the connectivity of the weak link network, giving a local field at the junctions of about 15 Oe. The approach yields a large value for the intragrain London penetration length, which matches with the strong intragrain granularity effects observed in Ru-1222.

#### ACKNOWLEDGMENTS

This work was partially supported by CNPq. S.G. was financed by FAPERJ.

\*Corresponding author. Electronic address: sgg@if.ufrj.br

- <sup>1</sup>L. Bauernfeind, W. Widder, and H. F. Braun, *Physica C* **254**, 151 (1995).
- <sup>2</sup>A. C. McLaughlin, W. Zhou, J. P. Attfield, A. N. Fitch, and J. L. Tallon, *Phys. Rev. B* **60**, 7512 (1999).
- <sup>3</sup>C. Bernhard, J. L. Tallon, E. Brücher, and R. K. Kremer, *Phys. Rev. B* **61**, R14 960 (2000).
- <sup>4</sup>R. S. Liu, L. Y. Jang, H. H. Hung, and J. L. Tallon, *Phys. Rev. B* **63**, 212507 (2001).
- <sup>5</sup>I. Felner, U. Asaf, and E. Galstyan, *Phys. Rev. B* **66**, 024503 (2002).
- <sup>6</sup>Y. Y. Xue, B. Lorenz, A. Baikalov, D. H. Cao, Z. G. Li, and C. W. Chu, *Phys. Rev. B* **66**, 014503 (2002).
- <sup>7</sup>G. V. M. Williams, L.-Y. Jang, and R. S. Liu, *Phys. Rev. B* **65**, 064508 (2002).
- <sup>8</sup>G. V. M. Williams, Ho Keun Lee, and S. Krämer, *Phys. Rev. B* **67**, 104514 (2003).
- <sup>9</sup>J. L. Tallon, C. Bernhard, and J. W. Loram, *J. Low Temp. Phys.* **117**, 823 (1999).
- <sup>10</sup>J. E. Croone, J. R. Cooper, and J. L. Tallon, *J. Low Temp. Phys.* **117**, 1199 (1999).
- <sup>11</sup>X. H. Chen, Z. Sun, K. Q. Wang, S. Y. Li, Y. M. Xiong, M. Yu, and L. Z. Cao, *Phys. Rev. B* **63**, 064506 (2001).
- <sup>12</sup>M. Pozek, A. Dulcic, D. Paar, A. Hamzic, M. Basletic, E. Tafra, G. V. M. Williams, and S. Krämer, *Phys. Rev. B* **65**, 174514 (2002).
- <sup>13</sup>M. Pozek, A. Dulcic, D. Paar, G. V. M. Williams, and S. Krämer, *Phys. Rev. B* **64**, 064508 (2001).
- <sup>14</sup>S. García and L. Ghivelder, *Phys. Rev. B* **70**, 052503 (2004).
- <sup>15</sup>I. Felner, E. Galstyan, B. Lorenz, D. Cao, Y. S. Wang, Y. Y. Xue, and C. W. Chu, *Phys. Rev. B* **67**, 134506 (2003).
- <sup>16</sup>S. García, J. E. Musa, R. S. Freitas, and L. Ghivelder, *Phys. Rev. B* **68**, 144512 (2003).
- <sup>17</sup>R. B. Goldfarb, A. F. Clark, A. I. Braginski, and A. J. Panson, *Cryogenics* **27**, 475 (1987).
- <sup>18</sup>F. Gömory and P. Lobotka, *Solid State Commun.* **66**, 645 (1988).
- <sup>19</sup>D. -X. Chen, R. B. Goldfarb, J. Nogués, and K. V. Rao, *J. Appl. Phys.* **63**, 980 (1988).
- <sup>20</sup>K. -H. Müller, *Physica C* **159**, 717 (1989).
- <sup>21</sup>M. Nikolo, L. M. Stacey, and M. J. Missey, *Physica B* **194–196**, 1875 (1994).
- <sup>22</sup>L. Ghivelder, I. Abrego Castillo, L. M. Pimentel, P. Pureur, and O. F. Schilling, *Physica C* **235–240**, 3221 (1994).
- <sup>23</sup>K. -H. Müller, M. Nikolo, and R. Driver, *Phys. Rev. B* **43**, 7976 (1991).
- <sup>24</sup>M. Nikolo and R. B. Goldfarb, *Phys. Rev. B* **39**, 6615 (1989).
- <sup>25</sup>K. -H Müller, *Physica C* **168**, 585 (1990).
- <sup>26</sup>M. Nikolo, *Physica B* **194–196**, 2129 (1994).
- <sup>27</sup>P. Pureur and J. Schaf, *J. Magn. Magn. Mater.* **69**, L215 (1987).
- <sup>28</sup>J. R. Clem, *Physica C* **153–155**, 50 (1988).
- <sup>29</sup>P. G. de Gennes, in *Superconductivity of Metals and Alloys* (W. A. Benjamin Inc., New York, 1966).
- <sup>30</sup>Y. Y. Xue, B. Lorenz, R. L. Meng, A. Baikalov, and C. W. Chu, *Physica C* **364–365**, 251 (2001).
- <sup>31</sup>A. Butera, A. Fainstein, E. Winkler, and J. Tallon, *Phys. Rev. B* **63**, 054442 (2001).